Constraints on the extragalactic magnetic field strength based on 145 months of Fermi-LAT observations and observable blazar spectrum modelling

Egor Podlesnyi, Timur Dzhatdoev, and Vladimir Galkin

The talk is based on our MNRAS paper. The code underlying the ELMAG extragalactic cascade simulations and the analysis is accessible on Zenodo.

Monthly Notices of the ROYAL ASTRONOMICAL SOCIETY

MNRAS **516,** 5379–5388 (2022) https://doi.org/10.1093/mnras/stac2509
Advance Access publication 2022 September 16

Constraints on the extragalactic magnetic field strength from blazar spectra based on 145 months of *Fermi*-LAT observations

E. I. Podlesnyi [1,2,3]★ T. A. Dzhatdoev [2,3] and V. I. Galkin [1,2]

[1] *Department of Physics, Federal State Budget Educational Institution of Higher Education M.V. Lomonosov Moscow State University, 1(2), Leninskie Gory, GSP-1, 119991 Moscow, Russia*
[2] *Skobeltsyn Institute of Nuclear Physics (SINP MSU), Federal State Budget Educational Institution of Higher Education M.V. Lomonosov Moscow State University, 1(2), Leninskie Gory, GSP-1, 119991 Moscow, Russia*
[3] *Institute for Nuclear Research of the Russian Academy of Sciences, 7a, 60th October Anniversary Prospect, 117312 Moscow, Russia*

$$\delta = \frac{D_e}{R_L} \simeq 3 \times 10^{-6}(1+z_{\gamma\gamma})^{-4} \left[\frac{B'}{10^{-18}\ \mathrm{G}}\right] \left[\frac{E'_e}{10\ \mathrm{TeV}}\right]^{-2}$$

$$\simeq 3 \times 10^{-6}(1+z_{\gamma\gamma})^{-2} \left[\frac{B_0}{10^{-18}\ \mathrm{G}}\right] \left[\frac{E'_e}{10\ \mathrm{TeV}}\right]^{-2}$$

Neronov & Semikoz (2009)

inverse Compton scattering on CMB

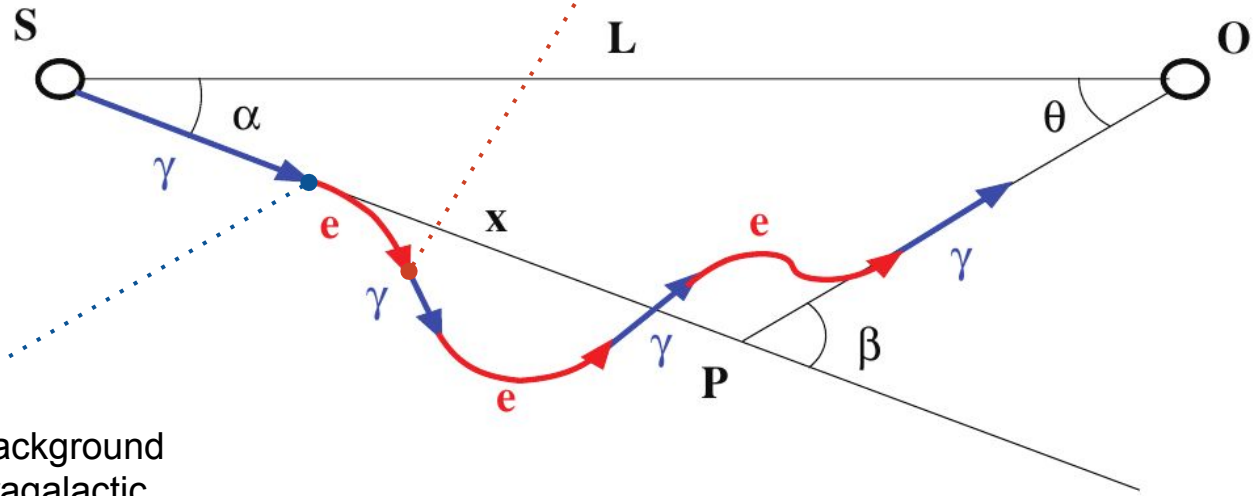

collision with the background photon of the Extragalactic Background Light (EBL), e^+e^--pair production (only electrons are shown)

Geometry of the extragalactic electromagnetic cascade

Dolag et al. (2009)

Contents lists available at SciVerse ScienceDirect

Computer Physics Communications

www.elsevier.com/locate/cpc

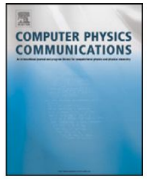

2012

ELMAG: A Monte Carlo simulation of electromagnetic cascades on the extragalactic background light and in magnetic fields ☆

M. Kachelrieß [a,*], S. Ostapchenko [a,b], R. Tomàs [c]

[a] Institutt for fysikk, NTNU, Trondheim, Norway
[b] D.V. Skobeltsyn Institute of Nuclear Physics, Moscow State University, Russia
[c] II. Institut für Theoretische Physik, Universität Hamburg, Germany

Used by Ackermann et al. (2018); simplified one-dimensional approach of the electron deflection angle calculation, small-angle approximation

Contents lists available at ScienceDirect

Computer Physics Communications

journal homepage: www.elsevier.com/locate/cpc

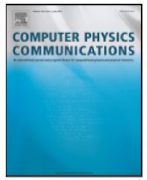

2020

ELMAG 3.01: A three-dimensional Monte Carlo simulation of electromagnetic cascades on the extragalactic background light and in magnetic fields ☆,☆☆

M. Blytt [a], M. Kachelrieß [a,*], S. Ostapchenko [b,c]

[a] Institutt for fysikk, NTNU, Trondheim, Norway
[b] Frankfurt Institute for Advanced Studies, Frankfurt, Germany
[c] D. V. Skobeltsyn Institute of Nuclear Physics, Moscow State University, Russia

Used by us; full three-dimensional approach of the electron deflection angle calculation, no small-angle approximation

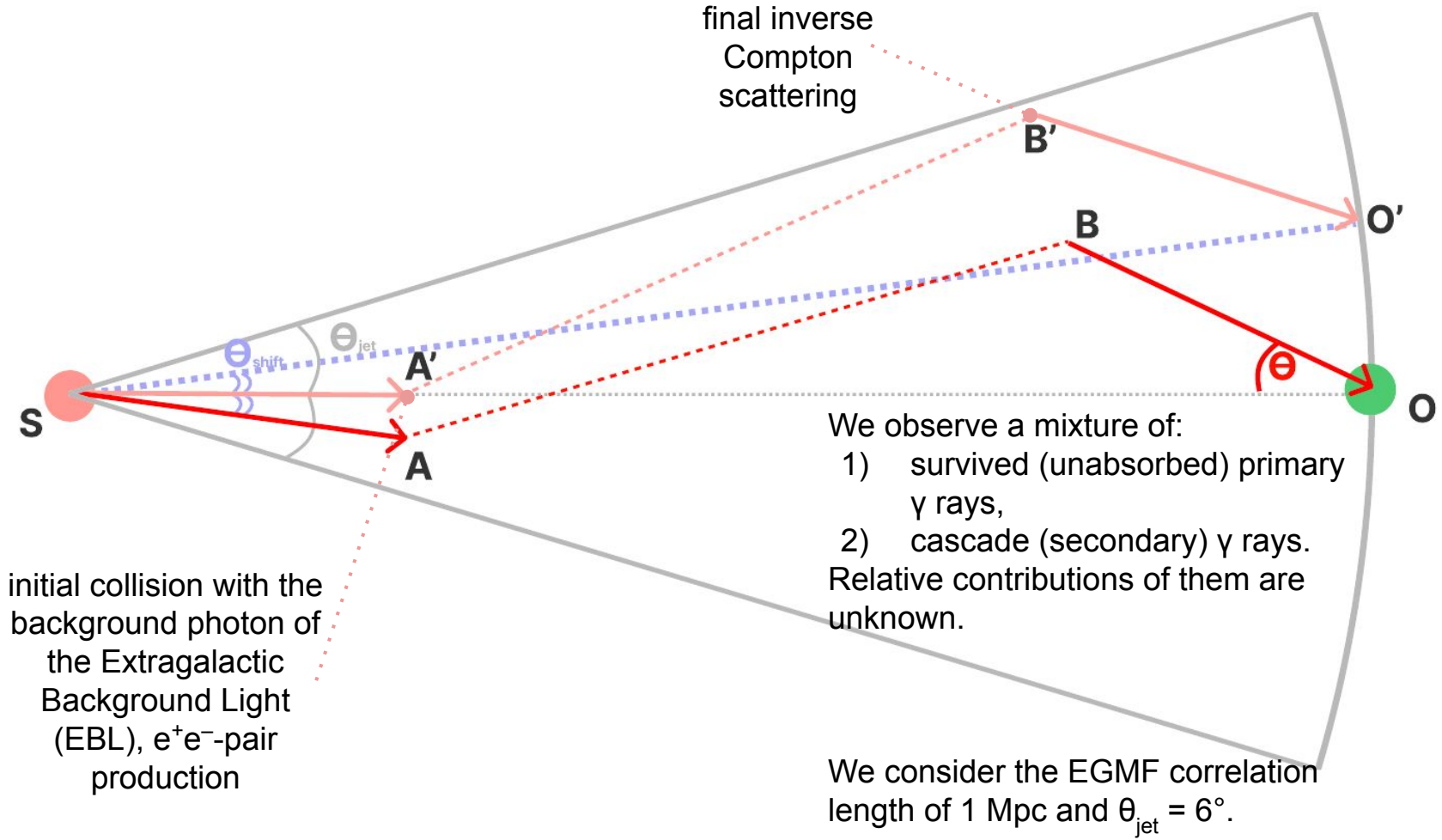
final inverse Compton scattering
B'
O'
B
θ
O
S
θshift
θjet
A'
A
initial collision with the background photon of the Extragalactic Background Light (EBL), e+e−-pair production
We observe a mixture of:
1) survived (unabsorbed) primary γ rays,
2) cascade (secondary) γ rays.
Relative contributions of them are unknown.
We consider the EGMF correlation length of 1 Mpc and θjet = 6°.

$$\Theta_{\rm ext} \simeq \begin{cases} 0.5^\circ (1+z)^{-2} [\frac{\tau_\theta}{10}]^{-1} [\frac{E_\gamma}{0.1\ {\rm TeV}}]^{-1} [\frac{B_0}{10^{-14}\ {\rm G}}], & \lambda'_B \gg D_e \\ 0.07^\circ (1+z)^{-1/2} [\frac{\tau_\theta}{10}]^{-1} [\frac{E_\gamma}{0.1\ {\rm TeV}}]^{-3/4} [\frac{B_0}{10^{-14}\ {\rm G}}] [\frac{\lambda_{B0}}{1\ {\rm kpc}}]^{1/2}, & \lambda'_B \ll D_e \end{cases}$$

Neronov & Semikoz (2009)

In basic instrumental observational gamma-ray analysis only those gamma-rays, which were detected inside the characteristic angular resolution $\Theta_{68\%}$, are attributed to the source of interest (point-source analysis). This spectral method is adopted in our work.

See, however, Manuel Meyer's presentation for the example of the full 2D angular-spectral analysis.

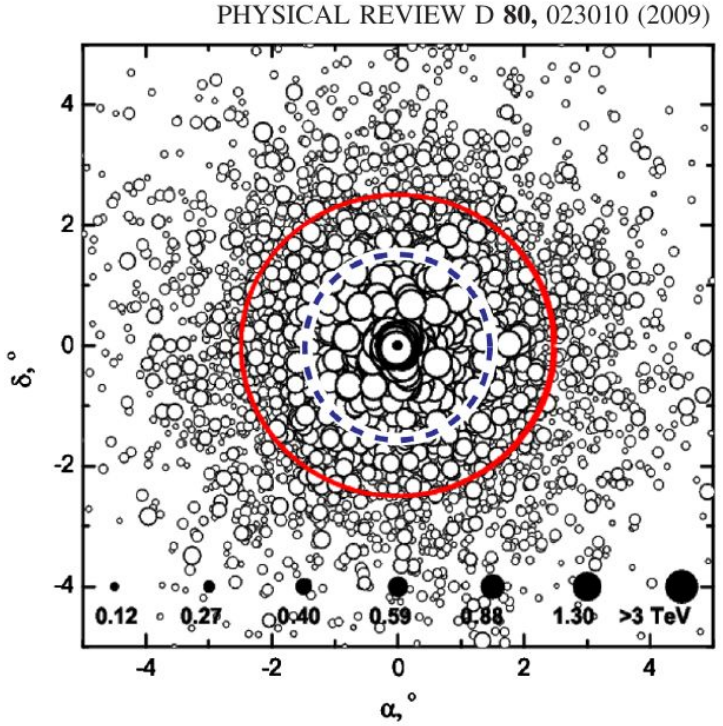

FIG. 4 (color online). The arrival directions of the primary and secondary cascade γ rays (circles) from a source at a distance $D = 120$ Mpc. The EGMF strength is 10^{-14} G. The sizes of the circles representing each photon are proportional to the photon energies. The blue dashed circle has radius 1.5°, equal to the radius of the FoV or MAGIC telescope. The radius of the red solid circle is 2.5°, which corresponds to the size of the FoV of the HESS telescope.

Elyiv et al. (2009)

ELMAG 3.01 output

$$A_{ijk}(E_i, E_{0_j}, \theta_k; B)$$

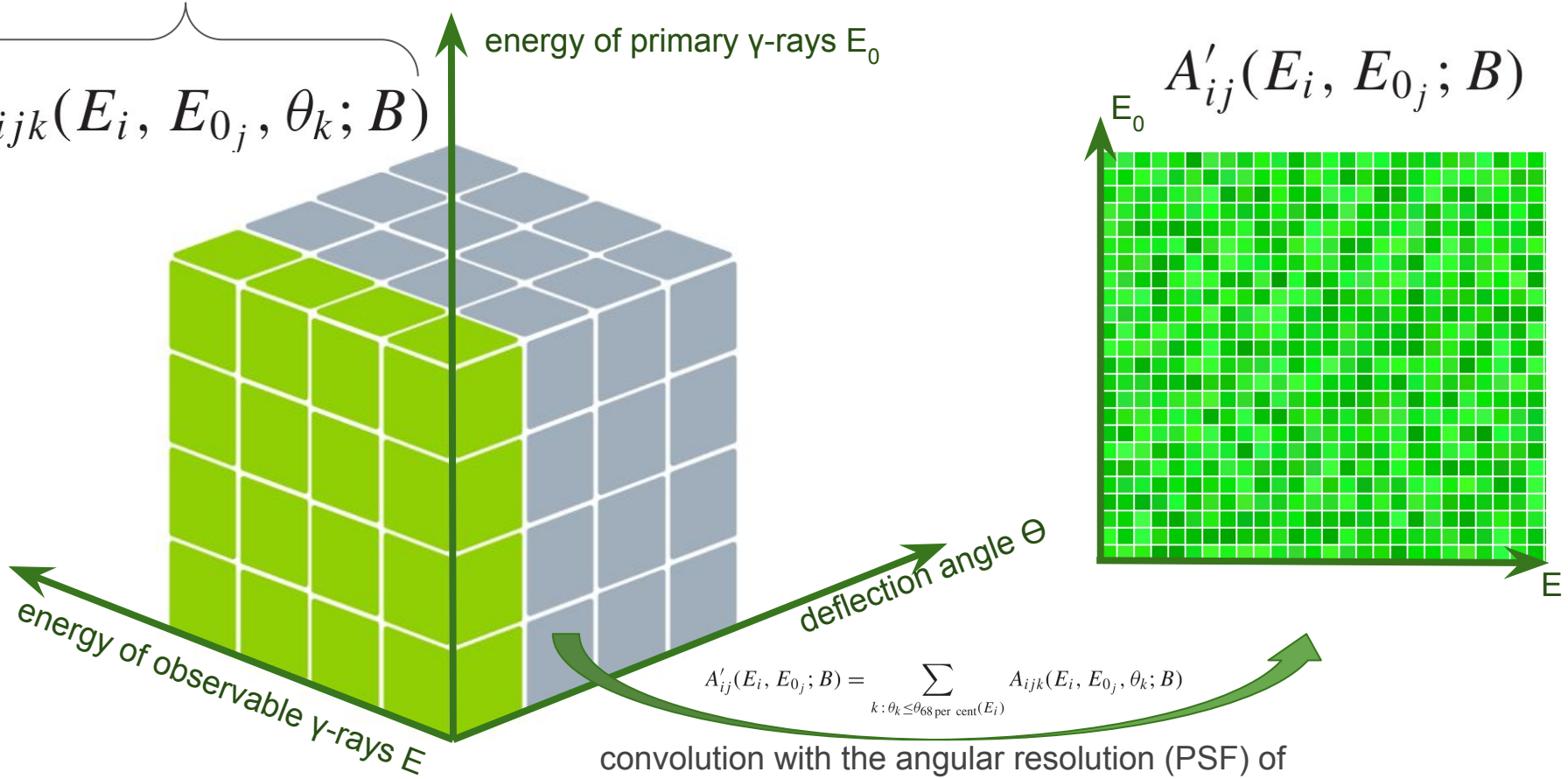

$$A'_{ij}(E_i, E_{0_j}; B)$$

$$A'_{ij}(E_i, E_{0_j}; B) = \sum_{k:\theta_k \le \theta_{68\,\mathrm{per\ cent}}(E_i)} A_{ijk}(E_i, E_{0_j}, \theta_k; B)$$

convolution with the angular resolution (PSF) of Fermi-LAT and IACTs (0.1∘)

$$A'_{ij}(E_i, E_{0_j}; B)$$

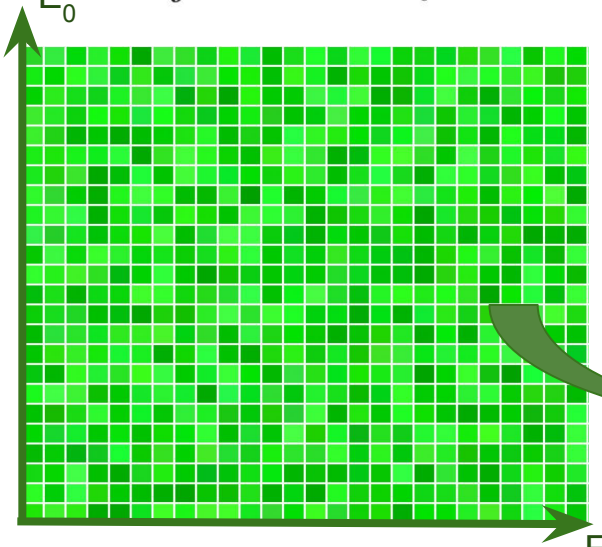

SED = E^2 dN / dE

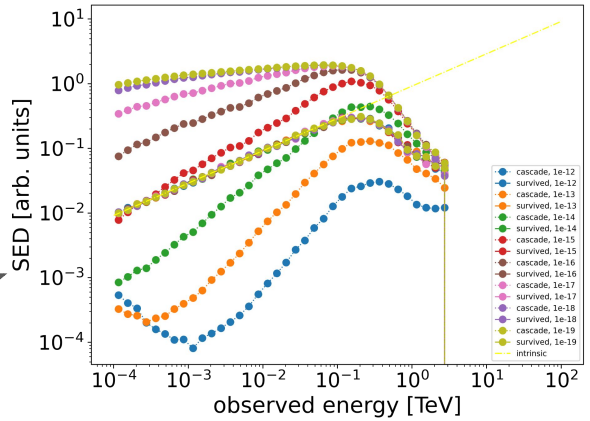

$$\frac{\mathrm{d}N}{\mathrm{d}E_i}(E_i; B; \boldsymbol{p}) = \sum_j A'_{ij}(E_i, E_{0_j}; B) W\left(E_{0_j}; \boldsymbol{p}\right)$$

profiling over source intrinsic spectrum parameters and convolving with the intrinsic spectrum with reweighting coefficients W

(i) Power law (PL):

$$\frac{\mathrm{d}N}{\mathrm{d}E_0} = C_0 \left(\frac{E_0}{E_{0_{\mathrm{ref}}}}\right)^{-\gamma_0}.$$

(ii) Power law with exponential cutoff (PLExp):

$$\frac{\mathrm{d}N}{\mathrm{d}E_0} = C_0 \left(\frac{E_0}{E_{0_{\mathrm{ref}}}}\right)^{-\gamma_0} \exp\left(-\frac{E_0}{E_{0_{\mathrm{cut}}}}\right).$$

(iii) Log-parabola (LP):

$$\frac{\mathrm{d}N}{\mathrm{d}E_0} = C_0 \left(\frac{E_0}{E_{0_{\mathrm{ref}}}}\right)^{-[\alpha_0+\beta_0 \ln(E_0/E_{0_{\mathrm{ref}}})]}.$$

(iv) Log-parabola with exponential cutoff (LPExp):

$$\frac{\mathrm{d}N}{\mathrm{d}E_0} = C_0 \left(\frac{E_0}{E_{0_{\mathrm{ref}}}}\right)^{-[\alpha_0+\beta_0 \ln(E_0/E_{0_{\mathrm{ref}}})]} \exp\left(-\frac{E_0}{E_{0_{\mathrm{cut}}}}\right).$$

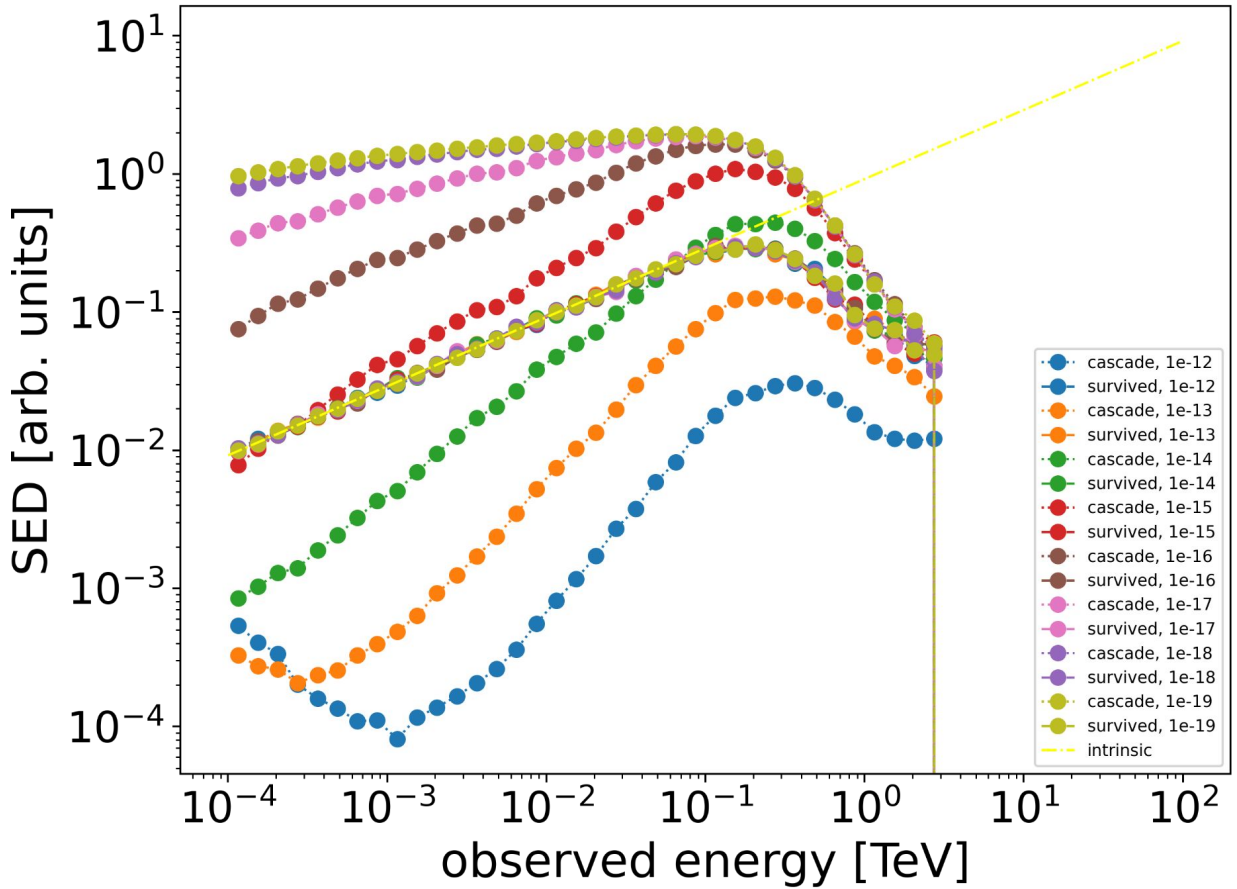

Spectral energy distribution (SED) examples for various strength of the EGMF observable with Fermi-LAT

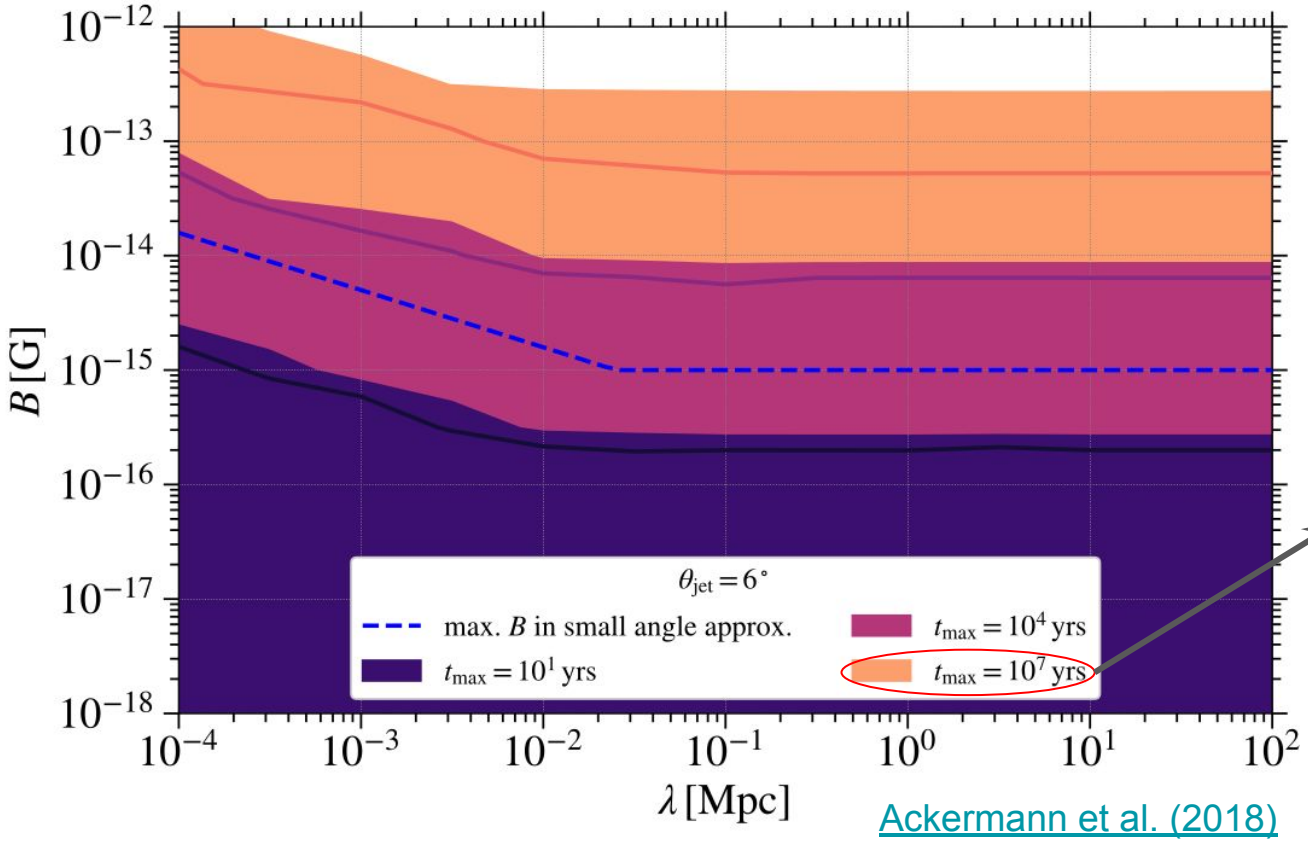

Ackermann et al. (2018)

Contemporary EGMF strength lower limits (95% CL) by Ackermann et al. (2018) are subject to critical assumptions, which, we believe, led the authors to the claimed values of the lower limits on the EGMF strength B.

We compare our results for the case of steady sources!

1. The source flux does not vary over the observation time and the IACT spectra are good representatives of the average flux level of the sources.
2. The intrinsic spectrum for each source over the whole *Fermi*-LAT and IACT energy range can be parameterized with a single LP function with exponential cutoff. The observed spectrum is then obtained by multiplying the intrinsic spectrum by the EBL absorption, which is parameterized through $\exp(-\tau(E, z))$, where $\tau(E, z)$ is the optical depth, which we assume to follow the model of Domínguez et al. (2011). The optical depth is a function of primary γ-ray energy and source redshift and is given by the same EBL model that we use for the ELMAG simulation. The observed spectrum is then given by the function

$$\phi_{\rm obs}(E, \boldsymbol{p}, z) = N(E/E_0)^{-(\alpha+\beta\ln(E/E_0))} \times \exp\left[-(E/E_{\rm cut} + \tau(E, z))\right], \quad (14)$$

   which has four free fit parameters, $\boldsymbol{p} = (N_0, \alpha, \beta, E_{\rm cut})$. We only assume concave spectra, i.e., $\beta \geqslant 0$ and set $E_0 = 1$ TeV throughout. Enforcing $\beta \geqslant 0$ should lead to conservative results for the cascade contribution, as it will decrease the intrinsic source flux at high energies.
3. Accounting for the cascade contribution does not change the best-fit spectrum of the central point source in the entire *Fermi*-LAT energy band by more than 5σ (see Section 2.5).
4. In each energy bin i, the spatial morphology of the cascade can be approximated using a 2D Gaussian halo component with a 68% containment radius equal to that of the cascade, i.e., $R_{{\rm halo},i} = R_{{\rm casc},i}$.
5. The cascade is not suppressed by the dissipation of energy of the e^+e^- beam into plasma instabilities (the efficiency of these instabilities is a matter of ongoing debate; see, e.g., Broderick et al. (2012); Sironi & Giannios (2014); Menzler & Schlickeiser (2015); and Chang et al. (2016)).

The cascade contribution is just a slight addition to the survived component of the observable SED

\+ neglection of the possible cascade contribution to the Imaging Atmospheric Cherenkov Telescopes (IACT) spectra

Some important assumptions by Ackermann et al. (2018)

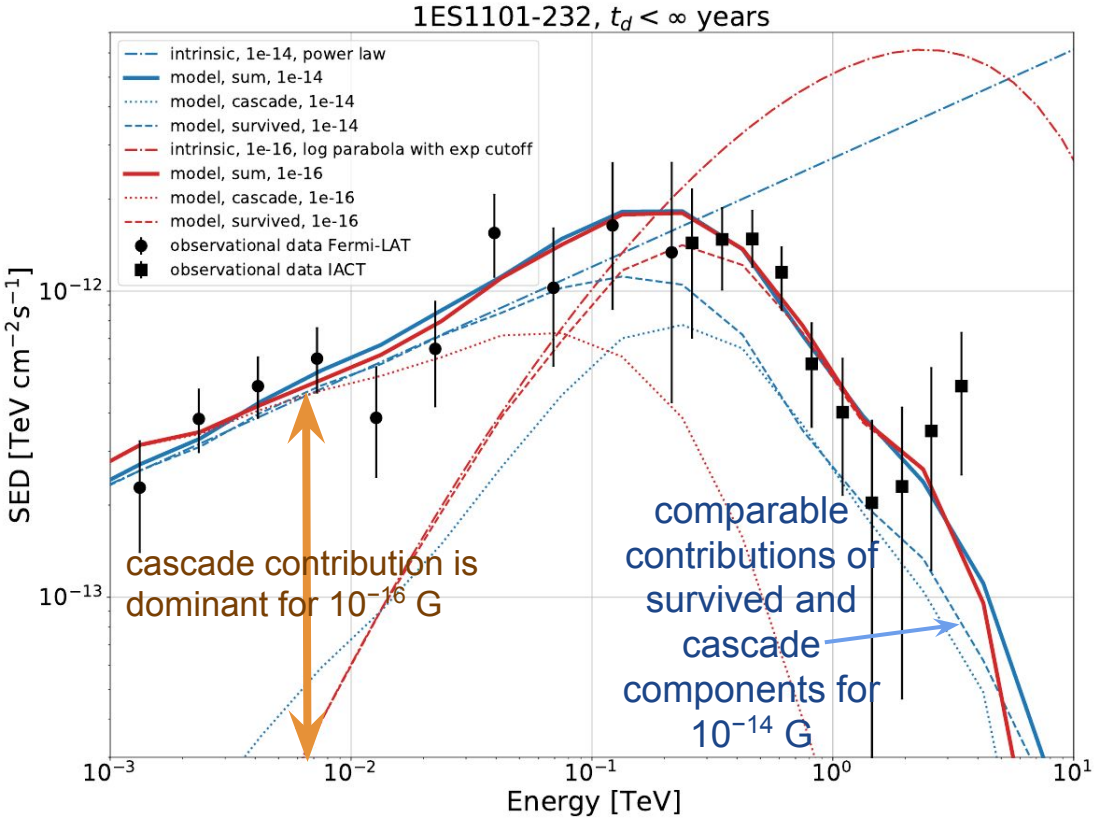

1ES 1101-232:
(i) power law & B = 10^{-14} G,
(ii) log parabola with *exp* cutoff & B = 10^{-16} G
give almost coinciding observable SEDs

In the range of 1–30 GeV in case i) the observable SED is dominated by the survived primary component. Contrary to case i), in case ii) the observable spectrum is dominated by more than one order of magnitude by the cascade component.

In case i), at the same time, the cascade and survived primary contributions are very similar at energies above 300 GeV.

Thus, assumptions of Ackermann et al. (2018) might be violated.

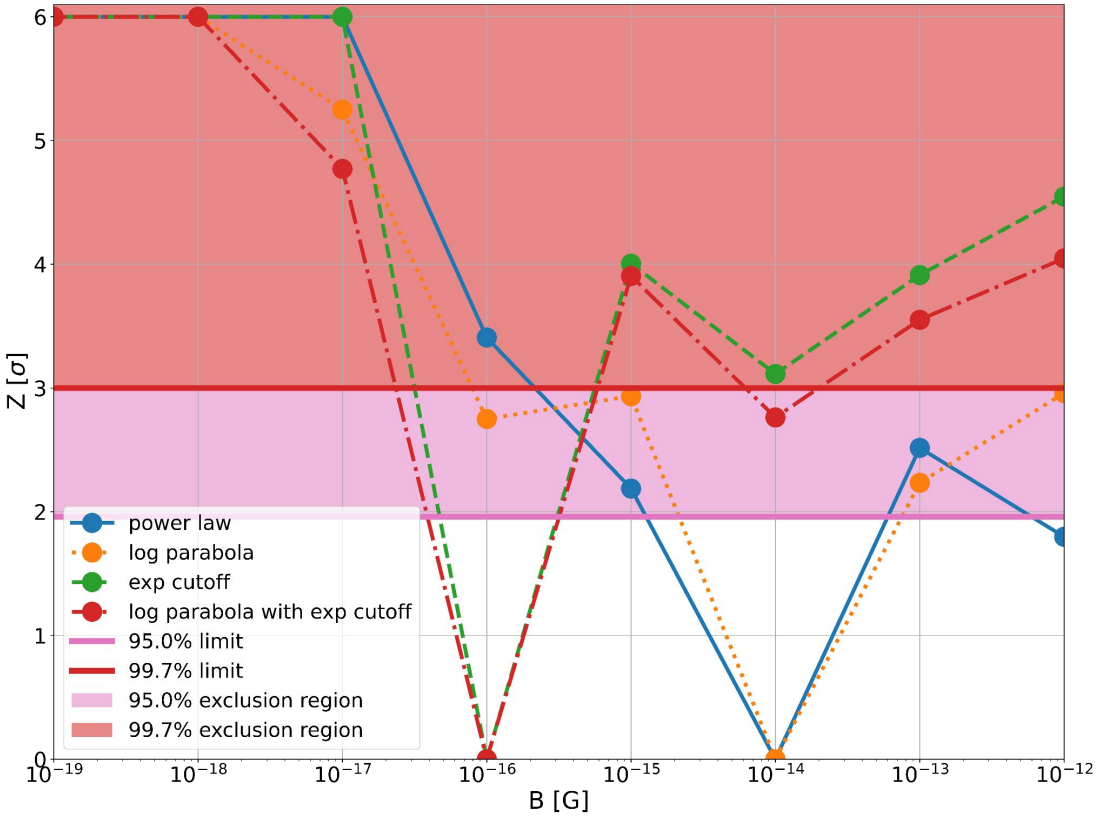

Based on combined measurements of 1ES 1218+304, 1ES 1101-232, and 1ES 0347-121, the EGMF strength values $B \leq 10^{-17}$ G are excluded at a high level of statistical significance $Z > 4\sigma$ for all the four options of the intrinsic spectral shape.

There are two best-fit solutions.

Contribution of cascade γ rays inside the Fermi-LAT PSF can be much greater than the contribution of survived γ rays.

Contribution of cascade γ rays to the IACTs SEDs should not be neglected.

$B = 10^{-16}$ G is a viable value of the EGMF strength.

Thank you for your attention!

This research was partly funded by the Interdisciplinary Scientific and Educational School of Lomonosov Moscow State University "Fundamental and Applied Space Research". The work of E.P. and T.D. on the VHE γ-ray propagation in the intergalactic medium was supported by the Russian Science Foundation, grant No. 22-12-00253.

Backup slides

Table 1. List of considered blazars, their 4FGL catalogue (Abdollahi et al. 2020) names, cosmological redshifts, IACT observational periods, and corresponding references. References for *z*: (1): Blanton et al. (2017) and Abdurro'uf et al. (2022); (2): Remillard et al. (1989); (3): Woo et al. (2005).

Source name	4FGL catalogue name	*z*; reference	IACT observational period(s)	Reference(s)
1ES 1218+304	4FGL J1221.3+3010	0.184; (1)	2012–2013	Madhavan (2013)
1ES 1101−232	4FGL J1103.6−2329	0.186; (2)	2004–2005	Aharonian et al. (2006, 2007a)
1ES 0347−121	4FGL J0349.4−1159	0.188; (3)	Aug.–Dec. 2006	Aharonian et al. (2007b)

Table 2. Main ELMAG 3 input parameters used in our simulations of extragalactic γ-ray propagation.

Parameter	Value
Source cosmological redshift	0.186
EBL model	Gilmore et al. (2012)
Minimal injection energy $E_{\rm MIN}$, eV	10^8
Maximal injection energy $E_{\rm MAX}$, eV	10^{14}
Power-law spectral index before the break	1.0
Power-law spectral index after the break	1.0
Jet opening angle $\theta_{\rm jet}$ in degrees	6.0
Jet misalignment angle $\theta_{\rm jetx}$ in degrees	0.0
Total number of injected primary γ-rays $n_{\rm max}$	60 000
Number of turbulent modes n_k	200
EGMF minimal spatial scale, Mpc	5×10^{-4}
EGMF maximal spatial scale, Mpc	5
EGMF correlation length λ, Mpc	1.0
EGMF root-mean-square strength B, G	$\{10^{-19}, 10^{-18}, 10^{-17}, 10^{-16}, 10^{-15}, 10^{-14}, 10^{-13}, 10^{-12}\}$

Systematic effects

(1) the uncertainty of the EBL models,
(2) unknown beaming pattern of the blazars, uncertainties of their jet opening and viewing angles,
(3) the unknown duty cycle of the sources,
(4) the uncertainty of the void filling factor (‘voidiness’),
(5) a possible contribution of cascades initiated by ultrahigh energy cosmic rays,
(6) Possible influence of the plasma energy losses,
(7) possible systematic shift in the SED measurements by Fermi-LAT and IACTs, stability of the TeV flux over the time activity (highlighted in the presentation by Paolo Da Vela)

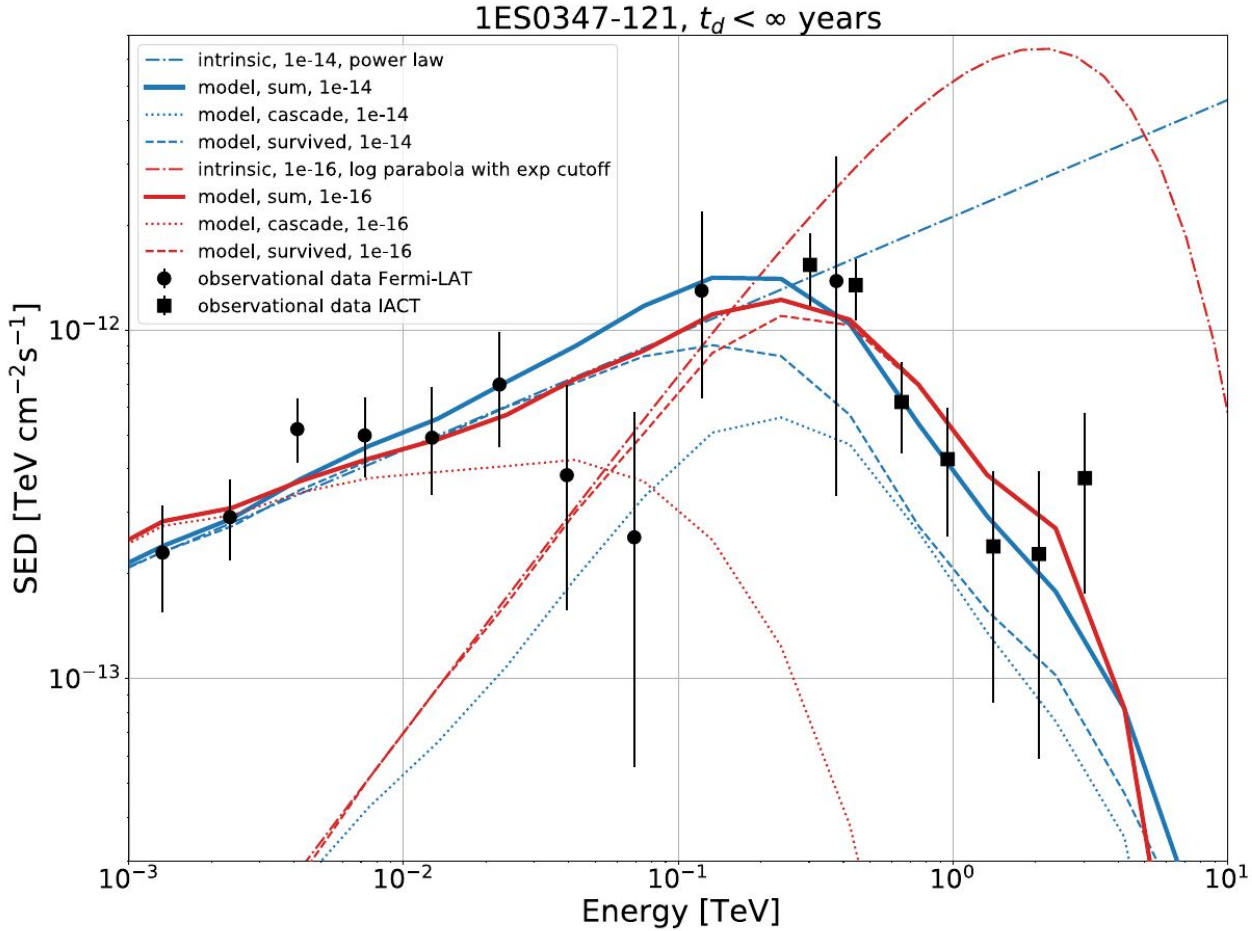

Figure A1. Example of the fitted SED of 1ES 0347−121 for two cases: (i) PL, $B = 10^{-14}$ G and (ii) LPExp, $B = 10^{-16}$ G.

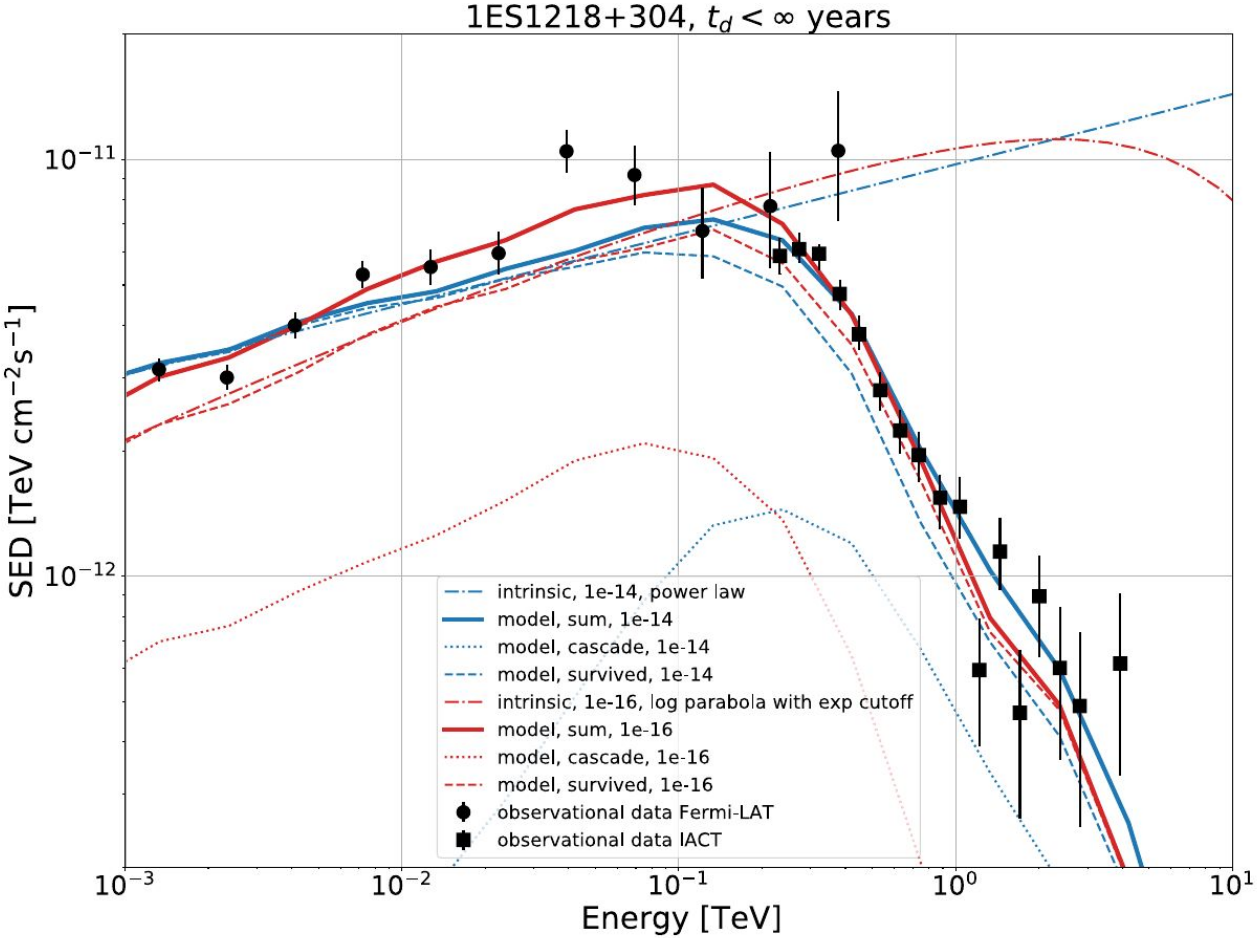

Figure A2. Example of the fitted SED of 1ES 1218+304 for two cases: (i) PL, $B = 10^{-14}$ G and (ii) LPExp, $B = 10^{-16}$ G.

$$\mathrm{TS}(B,\ \lambda) = -2\ln\left(\frac{\mathcal{L}(B,\ \lambda,\ \hat{\boldsymbol{p}}\,(B,\ \lambda))}{\mathcal{L}(\hat{\hat{B}},\ \hat{\hat{\lambda}})}\right)$$

Ackermann et al. (2018)

$$TS(B) = \chi^2(B;\ \hat{\boldsymbol{P}}(B)) - \min_{B}[\chi^2(B;\ \hat{\boldsymbol{P}}(B))]$$

Podlesnyi et al. (2022)

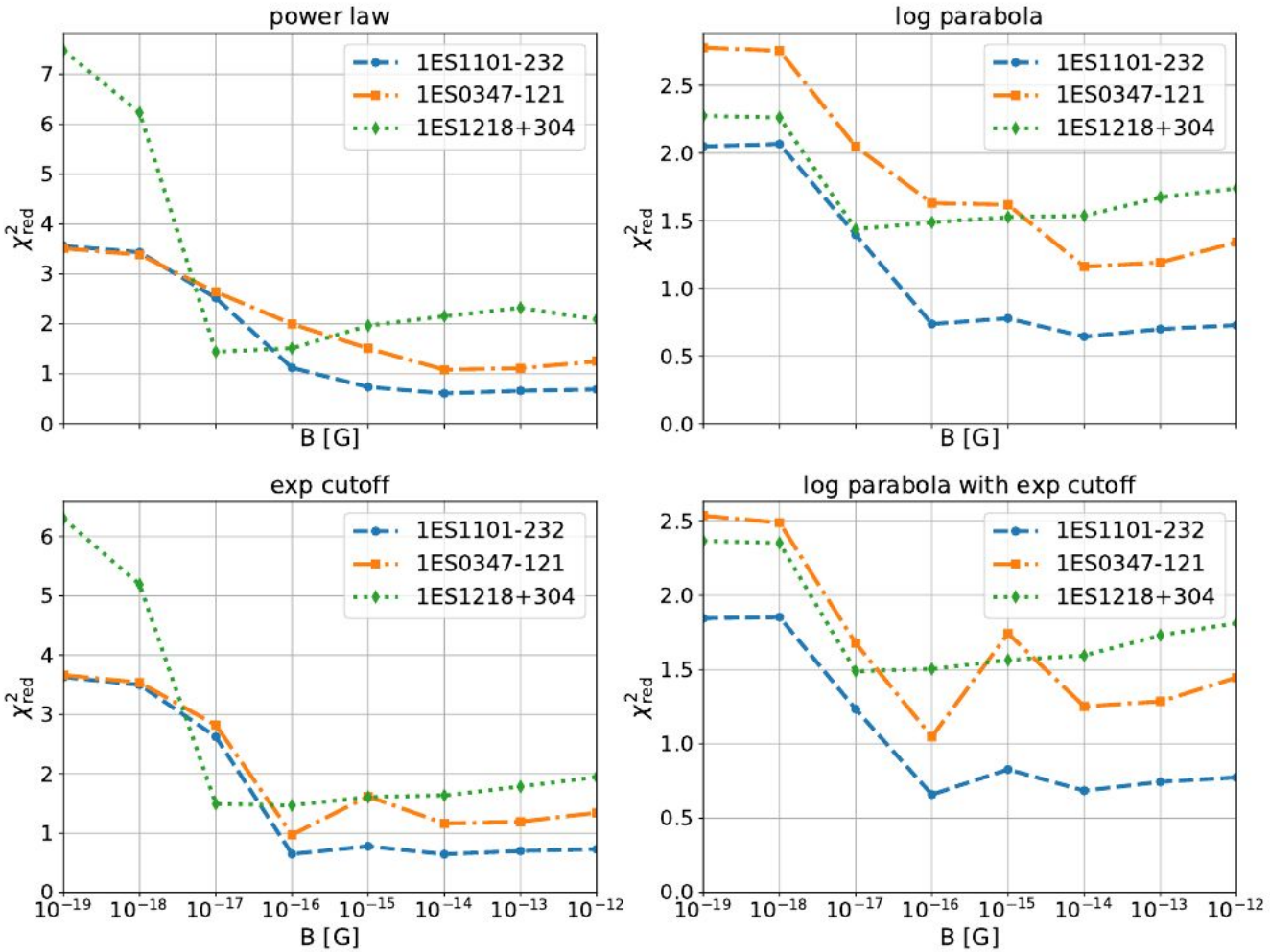
power law
log parabola
exp cutoff
log parabola with exp cutoff
1ES1101-232
1ES0347-121
1ES1218+304
χ^2_{red}
B [G]

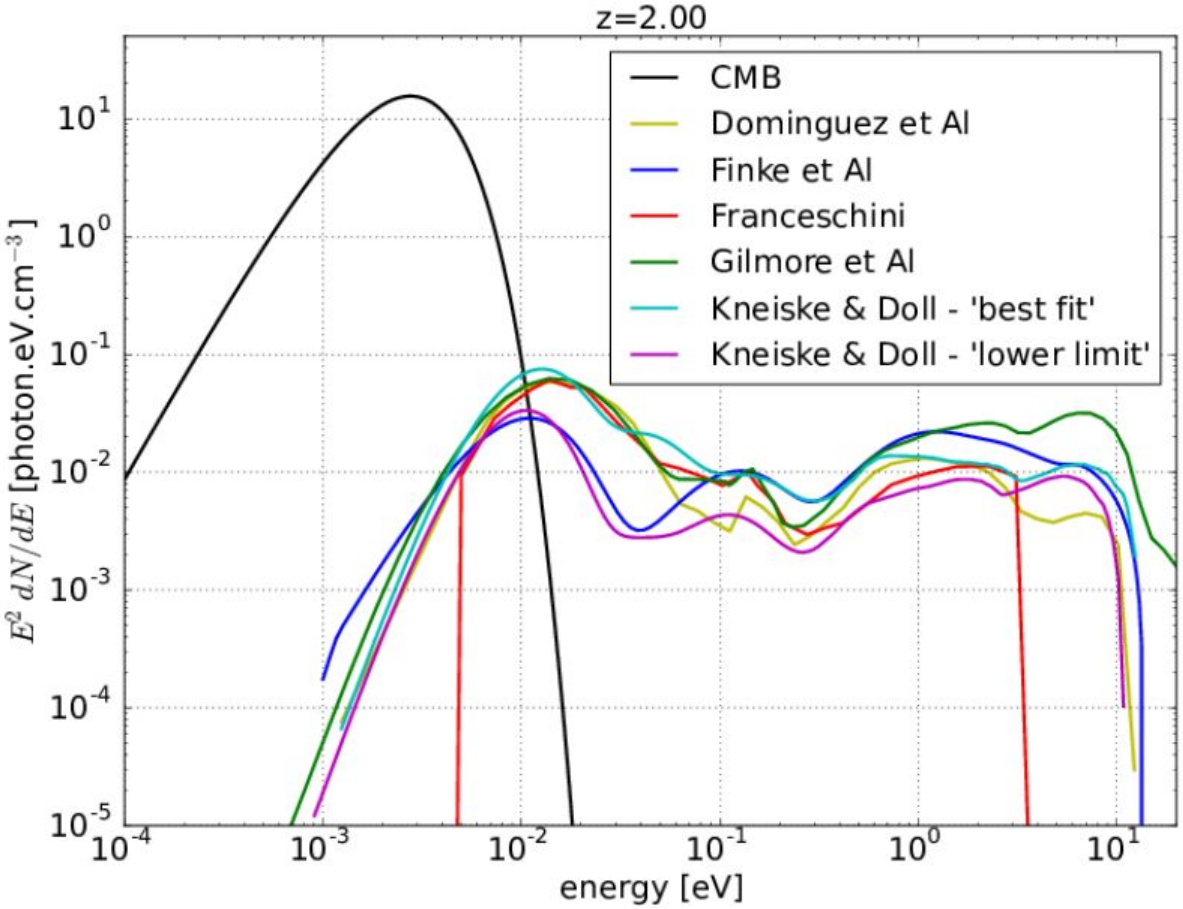

Monthly Notices of the Royal Astronomical Society, Volume 466, Issue 3, 21 April 2017, Pages 3472–3487

$$\Delta T = \sqrt{\Delta T_B^2 + \Delta T_P^2},$$

$$\Delta T_B = \frac{(1+z)L_\gamma}{2c}\left(1 - \frac{L_\gamma}{L_s}\right)\theta_B^2$$

$$\Delta T_P = \frac{(1+z)L_\gamma}{2c}\left(1 - \frac{L_\gamma}{L_s}\right)\theta_P^2$$

$$\theta_B \approx \frac{L_e}{R_L} \approx \frac{3\cdot 10^{-6}}{(1+z)^2}\left(\frac{B}{10^{-18}G}\right)\left(\frac{E_e}{10TeV}\right)^{-2}$$

For large values of the EGMF strength the corrected travel length can become negative ⇒ unexpected difference between 10^{-13} G and 10^{-12} G.

```
! correcting travel length
lar_rad=e0*1.081d0*3.086d0/(B_rms*2.d0/3.d0)/1.d3
xcorr=lar_rad*sin(x/lar_rad)
```